Journal of Orthopaedic Translation 29 (2021) 89–99

Contents lists available at ScienceDirect

Journal of Orthopaedic Translation

journal homepage: www.journals.elsevier.com/journal-of-orthopaedic-translation

Andrographolide attenuates synovial inflammation of osteoarthritis by interacting with tumor necrosis factor receptor 2 trafficking in a rat model

Rongliang Wang [a,b,1], Jiawei Li [a,b,1], Xingquan Xu [a,b], Jia Xu [b,c], Huiming Jiang [b,d], Zhongyang Lv [a,b], Rui Wu [a,b], Ziying Sun [a,b], Wenjie Guo [e], Yang Sun [e], Shiro Ikegawa [a,f], Qing Jiang [a,b,c,d], Dongquan Shi [a,b,c,d,*]

[a] State Key Laboratory of Pharmaceutical Biotechnology, Department of Sports Medicine and Adult Reconstructive Surgery, Nanjing Drum Tower Hospital, The Affiliated Hospital of Nanjing University Medical School, Nanjing, 210008, Jiangsu, PR China
[b] Joint Research Center for Bone and Joint Disease, Model Animal Research Center (MARC), Nanjing University, Nanjing, Jiangsu, 210093, PR China
[c] Drum Tower of Clinical Medicine, Nanjing Medical University, Nanjing, 210008, Jiangsu, PR China
[d] Department of Sports Medicine and Joint Surgery, The Affiliated Nanjing Hospital of Nanjing Medical University, Nanjing, 210000, PR China
[e] State Key Laboratory of Pharmaceutical Biotechnology, School of Life Sciences, Nanjing University, Nanjing, Jiangsu, 210093, PR China
[f] Laboratory for Bone and Joint Diseases, RIKEN Center for Integrative Medical Science (IMS, RIKEN), Tokyo, 108-8639, Japan

ARTICLE INFO

Keywords:
Andrographolide
TNFR2 trafficking
NF-κB
Synovial inflammation
OA treatment

ABSTRACT

Background: Synovial inflammation plays a major role in the pathogenesis of osteoarthritis (OA). This study investigated the effect of andrographolide (Andro) on synovial inflammation mediated by tumor necrosis factor-alpha receptor 2 (TNFR2) trafficking and its utility in attenuating OA progression.

Methods: Knee joints were harvested from rats subjected to radial transection of the medial collateral ligament (MCLT) and medial meniscus (MMT) to examine the effect of Andro on synovial inflammation and OA progression. Quantitative real-time polymerase chain reaction was used to evaluate the expression of inflammatory factors in primary fibroblast-like synoviocytes (FLSs) after Andro treatment *in vitro*. The mechanism underlying Andro-mediated regulation of TNFR2 distribution and nuclear factor-κB (NF-κB) expression was verified using endosome maturation inhibitor hydroxychloroquine (HCQ) through flow cytometry, immunofluorescence, and western blot analysis.

Results: Andro treatment was found to reduce synovial inflammation and OA progression *in vivo*. Furthermore, a decrease in pain hypersensitivity and dorsal horn neuron activation was observed after treatment. Andro also downregulated the expression of inflammatory mediators and TNFR2 in FLSs. TNFR2 is crucial for the activation of the NF-κB signaling pathway, and Andro-induced degradation of TNFR2 was associated with lysosomal function, which in turn, reduced the downstream phosphorylation of p65 in the NF-κB signaling pathway.

Conclusions: Andro could suppress synovial inflammation via regulation of TNFR2 trafficking and degradation. This also suggests it could be a potential treatment for the prevention of synovial inflammation and OA progression.

The translational potential of this article: This study provides strong evidence that Andro reduces NF-κB activation and inflammatory responses in OA FLSs via regulation of TNFR2 trafficking. The inhibition of TNFR2 and Andro could be a novel therapeutic approach for OA and pain management.

1. Introduction

Osteoarthritis (OA) is characterized by progressive degeneration of articular cartilage, synovial inflammation, joint pain and disability [1]. Various stressors, risk factors and genetics have been recognized; however, the pathological mechanism of OA remains poorly understood, as evidenced by a lack of effective therapeutic options [2]. Increasing evidence shows that synovial inflammation, and the resultant pro-inflammatory mediators, could accelerate the pathogenesis of OA

* Corresponding author. State Key Laboratory of Pharmaceutical Biotechnology, Department of Sports Medicine and Adult Reconstructive Surgery, Drum Tower Hospital, School of Medicine, Nanjing University, 321 Zhongshan Road, Nanjing, Jiangsu, 210008, PR China.
E-mail address: shidongquan@nju.edu.cn (D. Shi).
[1] These authors contributed equally to this work

https://doi.org/10.1016/j.jot.2021.05.001
Received 18 January 2021; Received in revised form 28 April 2021; Accepted 3 May 2021

Abbreviations

Andro	Andrographolide
TNFR	Tumor Necrosis Factor Receptor
NF-κB	Nuclear Factor Kappa-B
MCLT	Medial Collateral Ligament Transection
MMT	Medial Meniscus Transection
ADAMTS4	A Disintegrin and Metalloproteinase with Thrombospondin Motifs 4
ADAMTS5	A Disintegrin and Metalloproteinase with Thrombospondin Motifs 5
CCL2	Chemokine (C–C motif) Ligand 2
HCQ	Hydroxychloroquine

[3]. Almost 75% of all cells in the synovium are fibroblast-like synoviocytes (FLSs), and they are the major component of pathological synovial tissue [4]. Advances in synovial inflammation is closely related to synovial analgesia and structural modifications [5]. Additionally, inflammation in the joint that causes sensitization is thought to be the basis of arthritic pain [6]. Joint pain results from the activation of primary afferent nerve fibres in knee joint synovium [7], which expresses calcitonin gene-related peptide (CGRP), known to be involved in the transmission of nociceptive input to the cell bodies of sensory neurons located in the dorsal root ganglia (DRG) [8]. Hence, the molecular pathways that initiate synovial inflammation and novel treatment strategies targeting FLSs in OA processes urgently need to be investigated further.

Tumor necrosis factor-alpha (TNF-α) is one of the most potent pro-inflammatory cytokines and promotes OA progression and chronic joint pain [9]. It could activate nuclear factor-κB (NF-κB) signaling, a ubiquitous transcription factor widely involved in OA pathophysiology, through the stimulation of two distinct receptors: TNF receptor 1 (TNFR1) and TNF receptor 2 (TNFR2) [10]. Although these two receptors are both expressed in OA synovium [11], TNFR2 is less well characterized [12]; even its role in NF-κB signaling has rarely been described before [13]. Recent data has demonstrated a regulatory mechanism of receptor internalization and intracellular trafficking in selectively transmitting signals. Many internalized receptors from the cell surface are sorted to various intracellular compartments, like trans-Golgi vesicles or late endosomes, and then fuse with lysosomes and are proteolytically degraded [14]. TNFR1 was suggested to transduce death signals along this endosomal trafficking route [15]; however, it is unclear whether TNFR2 internalization is correlated with downstream signal transduction and could be used as a therapeutic target for OA synovial inflammation.

Andrographolide (Andro) is the main active constituent of *Andrographis paniculata* and exerts various pharmacological effects (e.g., antibacterial, anti-inflammatory, and anticancer effects) [16]. Studies have demonstrated that Andro, a well-known ent-labdane NF-κB inhibitor [17], can prevent the production of inflammatory and catabolic mediators by chondrocytes [18], suggesting that this natural compound has the potential to be a therapeutic drug for OA [19]. However, the mechanism by which Andro attenuates the progression of OA and synovial inflammation has yet to be elucidated. A recent study showed that Andro regulates cell surface expression and trafficking [20], providing a novel understanding of how Andro regulates NF-κB activation. Therapeutic effect mechanism of Andro on OA might be associated with the regulation of TNFR2 and downstream signal transduction in FLSs.

Therefore, the present study aimed to investigate the effect of Andro on TNFR2 trafficking in FLSs and the synovial inflammation in OA progression. Andro could be a promising drug for OA patients, and targeting TNFR2 has therapeutic potential for the clinical treatment of OA.

2. Materials and methods

2.1. Materials and reagents

Andro was obtained from Sigma–Aldrich (St Louis, MO, USA). Hydroxychloroquine (HCQ) was procured from Aladdin (Shanghai, China). Water-soluble Andrographolide sulfonate (Xi-Yan-Ping Injection) was provided by Jiangxi Qingfeng Pharmaceutical Co., Ltd (Jiangxi, China). GM6001 was purchased from MedChem Express (Monmouth Junction, NJ, USA). The IL-1β, IL-6 and TNF-α antibody were obtained from ABclonal (Wuhan, China). The primary antibodies against tumor necrosis factor-alpha receptor 2 (TNFR2), calcitonin gene-related peptide (CGRP), a disintegrin and metalloproteinase with thrombospondin motifs (ADAMTS)4, and ADAMTS5 were from Abcam (Cambridge, UK). The CCL2 antibody was obtained from Proteintech (Chicago, IL, USA). The PE-Phalloidin and goat anti-rabbit horseradish peroxidase (HRP)-labeled secondary antibody was obtained from Fude Biological Technology (Hangzhou, China). The antibodies against p-p65, p65, and GAPDH were obtained from Cell Signaling Technology (Danvers, MA, USA).

2.2. Animals

A total of 15 male Sprague–Dawley (SD) rats, 8-week-old, were purchased from the Laboratory Animal Center of Drum Tower Hospital, Nanjing, China. Before the experiments, all animals were housed, five per cage in regular cages at 24 °C under a 12-h light/dark cycle for 1 week, fed on commercial food and provided water.

2.3. Experimental protocol

All animal experiments complied with the guidelines of the Ethics Committee of Drum Tower Hospital, Medical School of Nanjing University, Nanjing, China (Ethics approval number: 2,018,020,004).

After acclimation, 10 rats underwent radial transection of the medial collateral ligament (MCLT) and medial meniscus (MMT) (MCLT + MMT) surgery on right knees [21], and 5 rats received sham operation. Briefly, the animals were anesthetized by subcutaneous administration of 30 mg/mL pentobarbital sodium before a medial patella arthrotomy was performed to expose the medial collateral ligament (MCL) and the central portion of the medial meniscus (MM). Then, a complete transection was performed in the MCL and MM. Subsequently, the OA rats were equally and randomly divided into two groups: MCLT + MMT group, and MCLT + MMT + Andro group. After the animals were left untreated for 1 week, Andrographolide sulfonate (10 mg/kg) in saline was injected intra-articularly in MCLT + MMT + Andro group rats twice a week. Rat in MCLT + MMT group were injected intraarticularly with same volume of saline (Fig. 1A).

2.4. Behavioral testing

Pain behavioral tests of rats from sham, MCLT + MMT and MCLT + MMT + Andro groups were performed on days 7, 14, 28 and 42 b y three independent examiners who were blinded to the experimental conditions (Fig. 1A). Mechanical withdrawal thresholds were assessed by application of an electronic von Frey Anaesthesiometer (IITC, Woodland Hills, CA, USA) according to the method described previously [22]. Briefly, rats were placed on a metal mesh floor, which allowed the tip of the anaesthesiometer to stimulate the mid-plantar aspect of the right hind paw. The paw withdrawal mechanical threshold (PWMT) was used by the "ascending stimulus" method [23] to record the tolerance level (in g), and calculated by averaging the data from the last three test.

The incapacitance testing, an index of joint discomfort in OA [24], consisted of placing the animal on an angled plate above an incapacitance meter that forced each hind paw on an independent pressure plate [25]. The force (g) exerted by each limb was measured and averaged over 5 s. The incapacitance score was reported as a percentage of

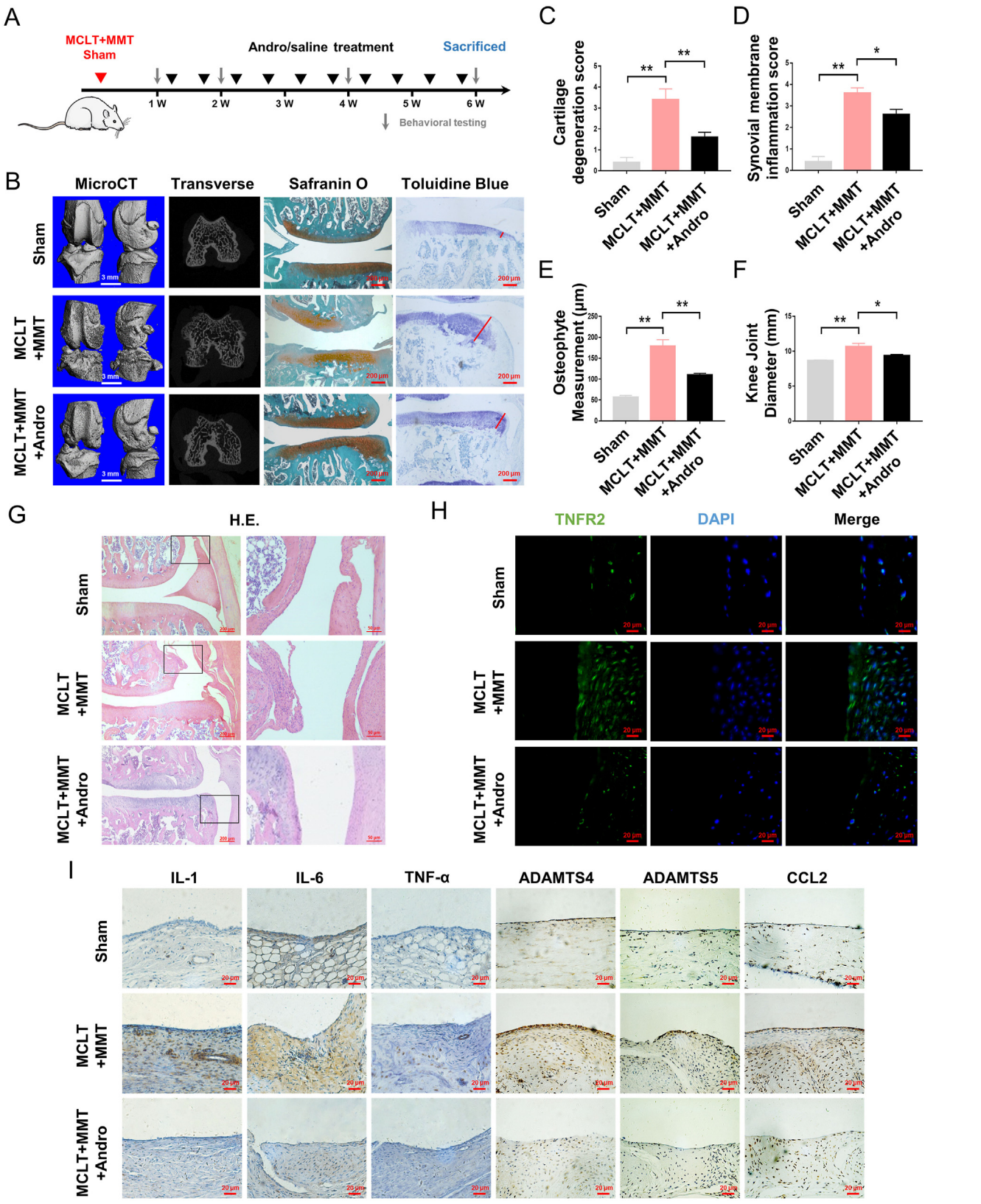

Fig. 1. Effects of Andro on the progression of OA *in vivo* (A) Schematic diagram of *in vivo* study (B) Three-dimensional micro-CT images of the knee joint (scale bar: 3 mm), histopathological safranin O, and toluidine blue staining (red line: measurement for the largest osteophyte) of knee joint sections in rats with MCLT + MMT following Andro treatment (scale bar: 200 μm) (C–E) Quantitation of cartilage degeneration, synovial inflammation and osteophyte measurement based on OARSI scores in rats with MCLT + MMT following Andro treatment (n = 5 rats/group) (F) Quantitation of knee joint diameter in rats with MCLT + MMT following Andro treatment (n = 5 rats/group) (G) Representative images of synovial membranes stained with H&E (scale bar: 200 μm and 50 μm) (H) Immunofluorescence of TNFR2 in the synovial membranes with MCLT + MMT following Andro treatment (Scale bar: 20 μm) (I) IHC of IL-1, IL-6, TNF-α, ADAMTS4, ADAMTS5, and CCL2 in the synovial membranes with MCLT + MMT following Andro treatment (scale bar: 20 μm). *$p < 0.05$; **$p < 0.01$.

the total weight bearing applied to the injured (right) hind paw based on the following formula: incapacitance score = right/(left + right) × 100.

A footprint analysis was performed the day before the end of the experiment. Evaluations were performed by dipping the posterior limb in red dye and the forelimb in black dye to calculate the median step width and length [19].

2.5. Microcomputed tomographic (micro-CT) analysis

At 6-weeks post-surgery, the rats were subjected to terminal anesthesia, perfused with heparinized saline through the left atrium, and fixed by 4% paraformaldehyde to harvest the lumbar spinal cords (20 mm) and knee joints. To perform 3D morphometric analysis of the knee joints, micro-CT scanning was performed using a micro-CT system (μCT-80, Scanco Medical, Bassersdorf, Switzerland). The X ray-tube was set at 70 kV and 114 mA for a resolution of 17.5 μm with an integration time of 250 ms. The 3D models of the harvested knee joints were determined with the original system of micro-CT following the manufacturer's protocols.

2.6. Histopathological analysis

Knee joints were fixed in 4% (v/v) paraformaldehyde for 24 h and then decalcified in 5% (v/v) EDTA for one month. Following dehydration in graded alcohol, the tissues were embedded in paraffin and sliced into 3-μm sagittal sections. To ensure that sections were coronal, the knee joint was carefully oriented using the shapes of the growth plates and menisci as hallmarks. The midcoronal sections of each joint were stained with safranin O, toluidine blue, and haematoxylin and eosin (H&E), which were used to evaluate Osteoarthritis Research Society International (OARSI) scores of cartilage degeneration, synovial inflammation and osteophyte measurement [26]. Briefly, OARSI scoring for cartilage degeneration is an evaluation of overall cartilage pathology, especially chondrocyte loss. The synovial inflammation score is based on increased numbers of synovial lining cell layers, proliferation of sub-synovial tissue, and infiltration of inflammatory cells. The largest osteophyte is measured by an ocular micrometer and the osteophyte OARSI scores are recorded as an average of the actual osteophyte measurement.

2.7. Immunohistochemistry (IHC) analysis

Bone sections were deparaffinized in xylene for 15 min, followed by rehydration using graded alcohol. Subsequently, endogenous peroxidase was blocked by 3% hydrogen peroxide for 20 min. After incubation with 0.4% pepsin (Aladdin) in 0.1 mM HCl at 37 °C for 60 min, the sections were blocked with 5% bovine serum albumin for 60 min and stained with IL-1β, IL-6, TNF-α, CCL2, ADAMTS4, and ADAMTS5 primary antibodies overnight at 4 °C and anti-rabbit/mouse secondary antibody at 37 °C for 3 h.

The lumbar spinal cords were fixed with 4% paraformaldehyde for 6 h for paraffin-embedding. The 3-μm sections were incubated with sodium citrate antigen retrieval solution (Servicebio, Wuhan, China) at 95 °C for 7 min and overnight with anti-CGRP at 4 °C. Finally, the sections were developed with chromogen for 10 min at 37 °C, dehydrated, and mounted for examination. All slides were visualized using a fluorescence microscope (Axio Observer A1, Zeiss, Germany).

2.8. Isolation and culture of human FLSs

FLSs were isolated from the resected synovial tissues of OA patients and this study was approved by the Ethics Committees of Drum Tower Hospital, Medical School of Nanjing University, Nanjing, China (Ethics approval number: 2,009,022). Briefly, the synovial tissues were minced into 1-mm pieces and treated with collagenase type I (Invitrogen, Carlsbad, CA, USA) at a concentration of 5 mg/mL in Dulbecco's modified Eagle's medium (DMEM) at 37 °C for 4 h. Subsequently, the cells were harvested by centrifugation at 1000×*g* for 5 min at 4 °C, and the pellet was resuspended in DMEM supplemented with 10% inactivated fetal bovine serum, 100 U/mL penicillin, and 100 mg/mL streptomycin at 37 °C in a 5% CO_2 atmosphere. FLSs at passages 2–4 were used for all experiments.

2.9. Cell proliferation assay

Briefly, FLSs (1×10^4 cells/cm^2) were seeded in a 96-well microplate for 24 h and exposed to Andro (0–90 μM) for an additional 24 h. The effects of Andro on the cell viability were assessed by CCK-8 (KeyGEN Biotech, Nanjing, China), according to the manufacturer's instructions. The absorbance (optical density) was measured at 450 nm and used as an index of cell proliferation and viability.

2.10. F-actin staining

FLSs (1×10^4 cells/cm^2) were plated in 96-well plates and cultured overnight, followed by 24-h exposure to various concentrations of Andro (0–90 μM). Then, the cells were fixed with 4% paraformaldehyde for 15 min and subjected to phalloidin staining in the dark. The expression of F-actin was observed by fluorescence microscopy. The morphological changes in the cytoskeleton were observed in at least three independent visual fields.

2.11. Western blotting

The treated FLSs (2×10^5 cells/cm^2) were lysed in radioimmunoprecipitation assay (RIPA) buffer, and proteins were isolated after centrifugation at 1000×*g* for 5 min at 4 °C. An equivalent of 20 μg of protein extract was separated using sodium dodecyl sulfate polyacrylamide gel electrophoresis (SDS-PAGE) and transferred to polyvinylidene difluoride membranes. The membranes were blocked with 5% non-fat milk for 1 h and probed with the appropriate primary antibodies overnight at 4 °C. Subsequently, the membrane was incubated with the secondary antibodies for 1 h. Finally, the immunoreactive bands were detected with an Enhanced Chemiluminescence Kit (Fude Biological Technology, Hangzhou, China) using the Tanon-5200 system (Biotanon, Shanghai, China).

2.12. Quantitative real-time polymerase chain reaction (qRT-PCR)

Total RNA was extracted using the RNA-Quick Purification Kit (ES Science, Shanghai, China), and complementary DNA (cDNA) was synthesized from 1 μg of extracted RNA using a HiScriptIIQ RT SuperMix for qPCR (Vazyme Biotech, Nanjing, China). The levels of the target transcript were calculated by $2^{-\Delta\Delta CT}$ method using SYBR Color qPCR Master Mix (Vazyme Biotech). The amplification and detection were carried out on a LightCycler 480-II (Roche, Mannheim, Germany). The primers are listed in Table 1.

2.13. Immunofluorescent staining

FLSs (5×10^4 cells/cm^2) are grown on coverslips, treated, washed in phosphate-buffered saline (PBS), and fixed in 4% paraformaldehyde for

Table 1
List of Primer Sequences used for qPCR.

Prime	Forward (5′-3′)	Reverse (5′-3′)
IL-1β	ATGATGGCTTATTACAGTGGCAA	GTCGGAGATTCGTAGCTGGA
IL-6	CCTGAACCTTCCAAAGATGGC	TTCACCAGGCAAGTCTCCTCA
TNFα	GAGGCCAAGCCCTGGTATG	CGGGCCGATTGATCTCAGC
ADAMTS4	GAGGGAGGCACCCCTAACT	CCTTGACGTTGCACATGGGA
ADAMTS5	GAACATCGACCAACTCTACTCCG	CAATGCCCACCGAACCATCT
CCL2	GCTCAGCCAGATGCAATCAATG	GTGTCTGGGGAAAGCTAGGG
GAPDH	ACAACTTTGGTATCGTGGAAGG	GCCATCACGCCACAGTTTC

20 min. Then, the cells were incubated with primary antibodies overnight at 4 °C, followed by staining with FITC- and TRITC-conjugated anti-rabbit/mouse antibody for 60 min at room temperature in the dark. The nuclei were counterstained with DAPI for 5 min, washed with PBST, and sealed with a coverslip. The images were captured by fluorescence microscopy.

2.14. Quantification of surface receptors

After treatment, FLSs (2×10^5 cells/cm^2) were blocked and probed with anti-TNFR2 primary antibody for 30 min. After washing several times with PBS, the stained cells were probed with a secondary anti-rabbit antibody for 15 min. Then, the cells were fixed with 2% paraformaldehyde and analyzed using a flow cytometer (BD FACSVerse, BD Bioscience, CA, USA).

2.15. siRNA transfection

The following siRNAs were designed and synthesized by Hippobio (Huzhou, China): siTNFR2 (s) 5′-CCGGCUCAGAGAAUACUAUTT-3′ (as) 5′-AUAGUAUUCUCUGAGCCGGCA-3'. The FLSs were cultured in 60-mm Petri dishes at a density of 2×10^5/mL for 48 h to reach 60–70% confluency and transfected using Lipofectamine 3000 siRNA reagent (Invitrogen, Carlsbad, CA, USA). The silencing efficiency was based on the mRNA determined by qPCR analysis.

2.16. Statistical analysis

The quantitative data were expressed as mean ± standard error of the mean (SEM). The statistical analysis of the parameters among the groups was conducted using SPSS statistical software program 20.0 (SPSS Inc., Chicago, IL, USA), and one-way analysis of variance (ANOVA) was used for multiple-group comparisons. P-value ≤ 0.05 indicated a significant difference.

3. Results

3.1. Andro attenuated cartilage wear and synovial inflammation during the progression of OA in vivo

To determine the effect of Andro alleviating OA and synovial inflammation *in vivo*, an intra-articular injection of Andrographolide sulfonate was performed on rat OA model. Safranin O and toluidine blue staining demonstrated the loss of proteoglycan (PG) and a decreased thickness in the medial and lateral aspects of rat articular cartilage induced by MCLT + MMT surgery. However, the percentage of PG and fibrillation in the articular cartilage surface was significantly higher in the Andro group compared to the MCLT + MMT group at the same time point (Fig. 1B), along with a lower OARSI scale of cartilage degeneration (Fig. 1C). Micro-CT imaging analysis and the actual osteophyte measurement revealed that MCLT + MMT injury increased the volume and surface area of osteophytes at both tibia and femur: changes in periarticular osteophytes were significantly improved by Andro treatment, compared to the MCLT + MMT group (Fig. 1B, E). After MCLT + MMT surgery, the knee joint diameter was increased in OA groups, whereas an intra-articular injection of Andro significantly reduced the knee diameter (Fig. 1F). Compared with the MCLT + MMT group, the infiltration of macrophages and OARSI score of synovial inflammation were significantly decreased in the Andro group (Fig. 1D, G). Along with decreased synovitis scores, the downregulation of TNFR2 and other inflammatory cytokines were also observed in the Andro-treated synovium (Fig. 1H and I).

3.2. Andro protected pain-like behavior of rats in OA

The relationship between joint damage and the gait pattern is measured by footprint analysis: this revealed that the track of animals from MCLT + MMT group was spatially asymmetric, with narrower step width and step length. However, animals in the Andro group showed consistent posterior limb coordination, with spatially symmetric step width and length compared to the sham group (Fig. 2A and B). Compared with the sham group at one week, a significant reduction was observed in the ipsilateral hindlimb weight-bearing of MCLT + MMT rats (approximately 15%), which declined by week six. Although no difference was detected in the early stage (<4 weeks), Andro treatment improved the incapacitance score at six weeks (approximately 10%), compared to the MCLT + MMT group (Fig. 2C). Similarly, the MCLT + MMT group was associated with the development of ipsilateral mechanical allodynia starting from week one up to week six, compared to the sham group. However, Andro treatment could significantly prevent the development of mechanical hypersensitivity in MCLT + MMT group rats from four weeks (Fig. 2D). Finally, an increased in CGRP expressing neurons was observed in the ipsilateral dorsal horn of the MCLT + MMT group and a decrease in the dorsal horn of Andro group. The density of CGRP expression was also significantly increased in the synovial tissue of the MCLT + MMT group near the blood vessels, while the density of CGRP$^+$ sensory nerves was reduced in the Andro group (Fig. 2E).

3.3. Andro suppressed cell viability and inflammatory expression in FLS

Andro treatment significantly decreased the proliferation of FLSs in, a dose-dependent manner (Fig. 3A). After 24 h of treatment, FLSs displayed abnormal distribution and structural damage of F-actin fibres, with a significant decrease in cell number (Fig. 3B). However, only a slight change in cell viability and morphology was observed at low Andro concentration (10 and 30 μM). mRNA expression of inflammatory factors *IL-1β*, *IL-6*, *CCL2*, *ADAMTS4*, and *ADAMTS5* was significantly increased in response to TNFα stimulation, whereas, the putative inhibitory effects of Andro on TNFα-stimulated OA-FLSs resulted in a significant reduction in the expression of these inflammatory markers (Fig. 3C). After treatment with Andro, FLSs also showed a significant decrease in *IL-1β*, *IL-6*, *TNFα*, *CCL2*, *ADAMTS4*, and *ADAMTS5* expression, in a dose-dependent manner (Fig. 3D). Based on these findings, 30 μM concentration of Andro was used in the following experiments.

3.4. Andro-regulated TNFR2 expression in vitro

Western blot analysis showed that TNFR2 expression was downregulated after 30 μM Andro treatment, in a dose-dependent manner (Fig. 4A). The decreased TNFR2 was effectuated in a time-dependent manner (Fig. 4B). Under normal condition, TNFR2 was uniformly distributed in FLS cells; whereas treatment with 30 μM Andro caused a significant change, with TNFR2 accumulating around the perinuclear region (Fig. 4C). Correspondingly, an increase in TNFR2 expression after TNF-α stimulation was likely reversed by treatment with Andro (Fig. 4D). However, the qPCR data did not reveal any change in the amount of *TNFR2* mRNA at the transcriptional level post-Andro treatment (Fig. 4E). Approximately 10% of surface TNFR2 was downregulated after treatment with Andro: only HCQ could reverse this effect. GM6001 appeared to have no significant effect on the surface expression of TNFR2 in Andro-treated cells (Fig. 4F). HCQ also increased the protein level of TNFR2 in Andro-stimulated FLSs (Fig. 4G). A co-localisation study to determine the final compartment that TNFR2 accumulated in after Andro treatment, identified that TNFR2 co-localised with lysosomal-associated membrane protein-1 (LAMP-1) in the perinuclear compact membrane structure in Andro group compared with control. However, this trafficking and co-location could be blocked after HCQ treatment (Fig. 4H).

3.5. Andro inhibited the activation of NF-κB signaling via TNFR2

Western blot analysis of FLSs revealed that TNFα induced p65 phosphorylation, but this effect was reduced in both Andro-treated groups

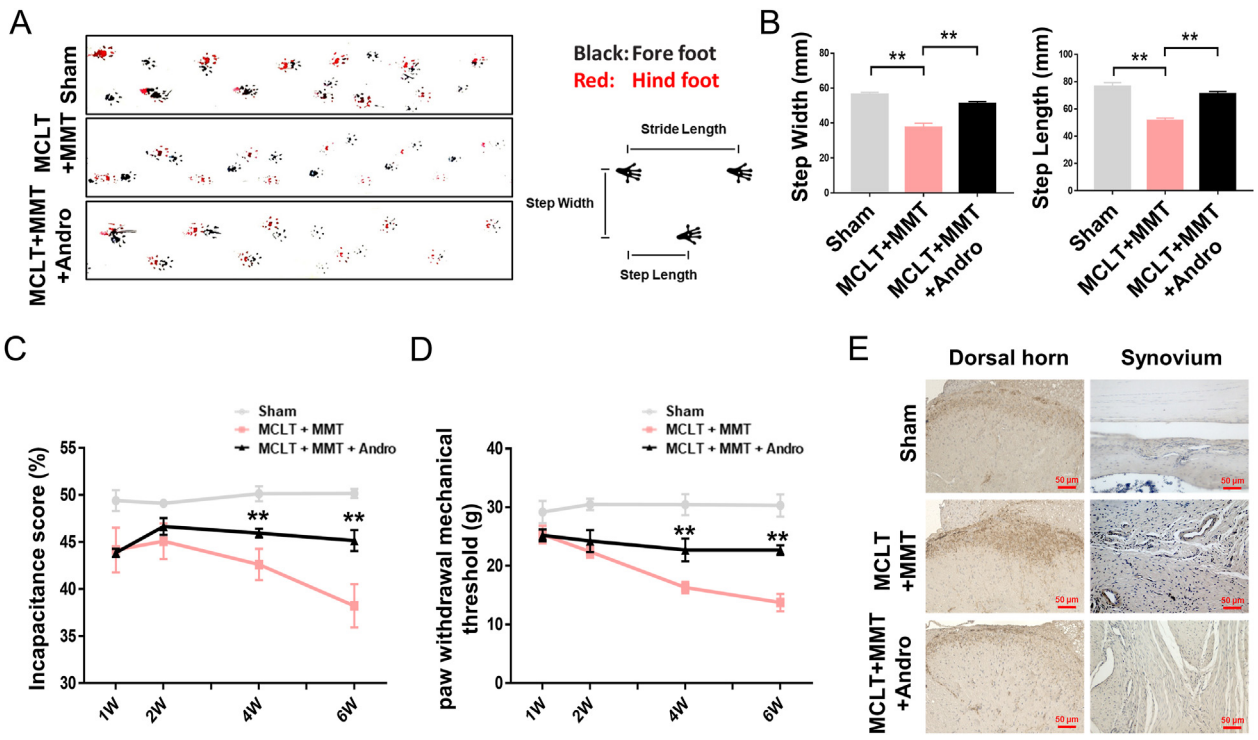

Fig. 2. Effects of Andro on pain-like behavior of OA *in vivo* (A, B) Footprint analysis results of different groups and common spatial characteristics of the rat, including step width and step length (C) Pain testing assessed as incapacitance analgesia meter in rats with MCLT + MMT following Andro treatment (n = 5 rats/group) (D) Changes of pain sensitivity after MCLT + MMT surgery with/without Andro treatment determined by measuring the paw withdrawal mechanical threshold (n = 5 rats/group) (E) IHC of CGRP in the dorsal horn and synovial membranes with MCLT + MMT following Andro treatment (scale bar: 50 μm). **p < 0.01.

(Fig. 5A). Immunofluorescence studies indicated that cells stimulated with TNFα showed an increase in the nuclear translocation of p65 from the cytoplasm, while those treated with Andro showed less nuclear translocation (Fig. 5B). To verify the involvement of TNFR2 in TNFα/NF-κB (p65) signaling, si-TNFR2 was first found to be no effect on the basal production of p-p65, but TNFα-induced p65 phosphorylation declined two-fold in FLSs transfected with the TNFR2-siRNA. Similarly, TNFα-induced p-p65 production by Andro was suppressed significantly after FLSs were transfected with the siRNA (Fig. 5C and G). Surface TNFR2 is required for p65 phosphorylation, therefore, restoring TNFR2 via HCQ treatment increased production of p-p65 in Andro-treated cells (Fig. 5D) and the levels of p65 in the nuclear compartment of Andro-treated FLSs (Fig. 5E). In addition, the production of pro-inflammatory cytokines was also enhanced in the HCQ-treated group, with higher levels of *ADAMTS4*, *ADAMTS5*, and *CCL2* mRNAs than the Andro-treated group (Fig. 5F).

4. Discussion

This is the first time the role of Andro in regulating TNFR2 trafficking has been investigated as a therapeutic approach for treating synovial inflammation in the pathogenesis and development of OA. Andro significantly reduced synovitis-associated inflammation and attenuated cartilage degeneration, osteophyte formation, and joint pain in an experimental rat OA model. Furthermore, the anti-inflammatory effect of Andro was due to the regulation of TNFR2 trafficking and degradation, which was indispensable for NF-κB inhibition in FLSs (Fig. 6).

Andro is a potential anti-inflammatory drug that disrupts the inflammatory response in FLSs to attenuate OA progression. Synovial inflammation is frequently involved in the progression of OA [27], and FLSs can secrete a large number of inflammatory cytokines and mediators, accelerating OA progression [28]. Some chemokines, such as IL-1β, IL-6 and TNFα, can attract other immune cells to accumulate around articular cartilage, resulting in an inflammatory environment that induces chondrocytes to secrete cartilage-degrading enzymes and proteases [29]. ADAMTS activity has been shown to degrade cartilage proteoglycan-aggrecan in arthritis [30], and CCL2 is also an important factor that modulates monocyte/macrophage recruitment in OA [31]. In this study, Andro downregulated the expression of pro-inflammatory cytokines, such as *IL-1β*, *IL-6*, *TNFα*, *CCL2*, *ADAMTS4* and *ADAMTS5*. Thus, Andro-induced inhibition of OA inflammation might be related to decreased levels of these inflammatory mediators in OA FLSs. In addition, the proliferation of FLSs plays a significant role in the production of inflammatory cytokines [32]. Andro also inhibited growth and invasion by modulating cell proliferation and cytoskeletal rearrangement in FLSs, which was consistent with the findings of previous studies [33,34]. Hence, Andro-induced suppression of the inflammatory response in OA FLSs is reported for the first time, and Andro is identified as a promising therapeutic agent for treating and preventing inflammation in OA [19].

Andro was also found to be a potential analgesic drug for OA pain. CGRP is widely expressed in the central and peripheral nervous systems and plays a role in OA pain processes [35]. Andro treatment suppressed the enhancement of $CGRP^{+}$ sensory nerves in the lumbar spinal cords and synovial tissues during OA, indicating that Andro treatment improved pain behavior, and both central and peripheral sensitization by blocking the spread of pain to sites distant from the joint [36,37]. Peripheral sensitization is a principal contributor to arthritis-related pain, and this pain development largely depends on the interaction between the immune response and the distal endings of joint-innervating DRG sensory neurons in the knee joint [38,39]. FLSs, and the inflammatory mediators they secrete, promote peripheral sensitization [40]. For example, an anti-ADAMTS5 antibody was found to influence mechanical allodynia in the medial meniscus (DMM) model [41], and $CCL2^{-/-}$ DMM model mice also showed delays in the development of pain-related behaviour [42]. Increased expression of ADAMTS5 and CCL2 was observed in the synovial tissues of OA rats, which could be recovered by Andro administration. Thus, Andro-mediated inhibition of these inflammatory cytokines and chemokines highlights the analgesic effect of Andro on OA pain.

Furthermore, Andro induced TNFR2 trafficking for lysosomal

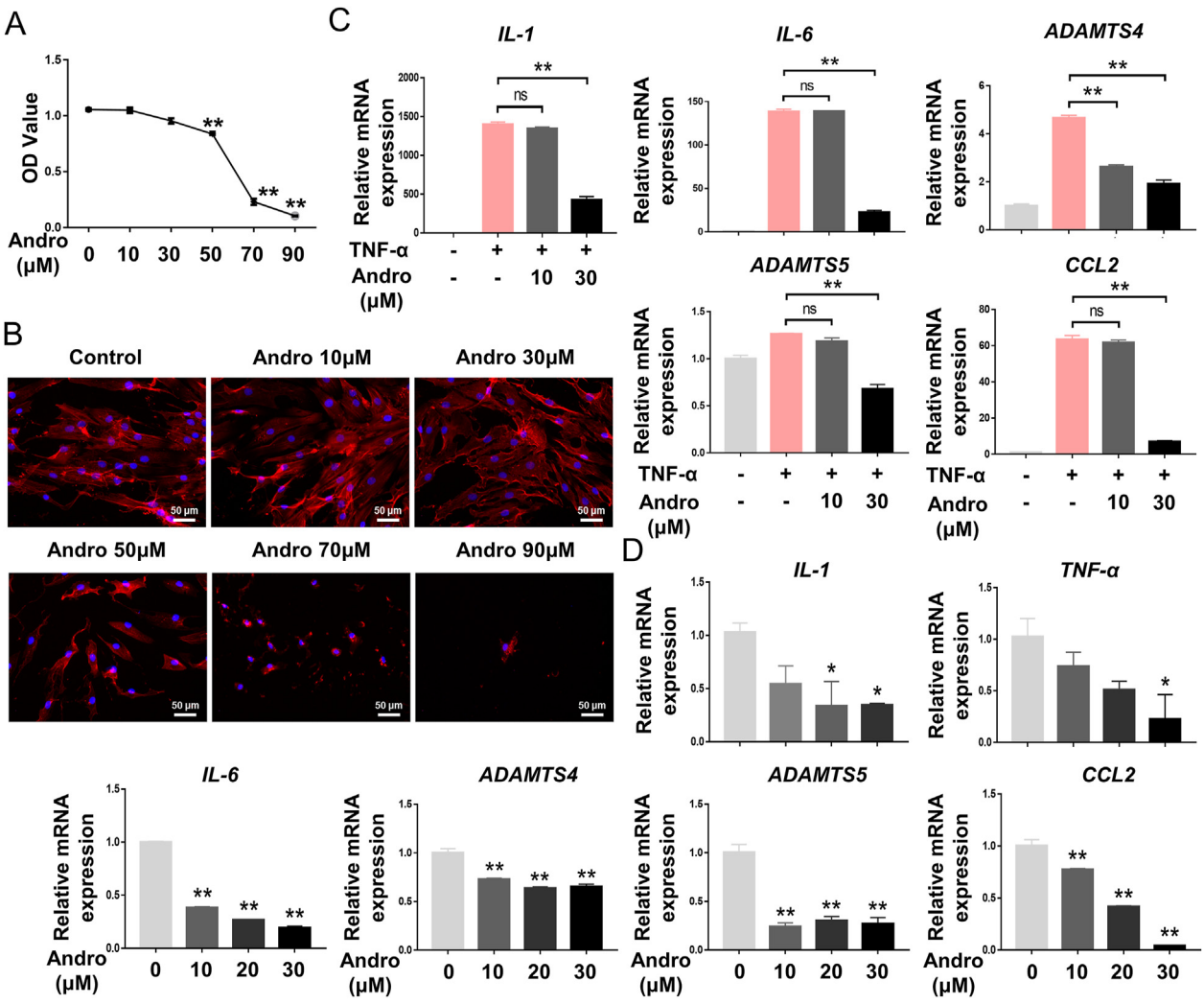

Fig. 3. Effects of Andro on cell viability and inflammatory expression in FLS (A) CCK-8 assay showed the effect of Andro on cellular proliferation at the concentrations used (0–90 μM) following treatment for 24 h (B) FLSs treated with different concentrations (0–90 μM) of Andro showed changes in cell morphology and cytoskeletal structure (C) mRNA expression of the inflammatory cytokines under the stimulation of TNFα (10 ng/mL) in FLSs with/without Andro for 24 h (n = 3) (D) mRNA expression of the inflammatory cytokines under the treatment of Andro in FLSs for 24 h (n = 3). ns, $p > 0.05$, *$p < 0.05$; **$p < 0.01$.

degradation and depleted functional TNFR2. First, TNFR2 was rapidly downregulated and then accumulated in the perinuclear region after Andro treatment. Previous studies have confirmed that metalloprotease-dependent shedding and internalization contribute to transient receptor clearance from the cell surface [43,44]. Thus, an assessment of which regulation was necessary for Andro-induced inhibition of TNFR2 expression was made. For this purpose, FLSs were pretreated with HCQ, an inhibitor of receptor internalization [45], and the metalloprotease inhibitor GM6001 to monitor the surface receptor expression of TNFR2 by flow cytometry analysis. Metalloprotease activity was found to exert no effect on Andro-induced downregulation of surface TNFR2 in this study. However, HCQ reversed the Andro-induced upregulation of surface TNFR2 expression. Thus, it could be deduced that Andro affected the trafficking machinery involved in internalizing cell surface TNFR2, which is similar to previous findings on Andro-mediated regulation of EGFR on the cell surface and degradation [20]. Receptor internalization results in transient receptor clearance from the cell surface, followed by either recycling to the membrane or lasting clearance through degradation in lysosomes [46]. Hence, it was determined that, in the presence of Andro, TNFR2 accumulated in compartments that were positive for LAMP-1, a commonly used marker for both late endosomes and lysosomes [47]. HCQ-induced inhibition of the lysosomal degradation of TNFR2 could eventually enhance the surface expression of TNFR2 on Andro-treated FLSs. Therefore, the present study shows, for the first time, that Andro induces TNFR2 trafficking and degradation by accelerating the movement of the receptor from the cell surface to late endosomes and lysosomes.

Andro-induced inhibition of TNFR2 and NF-κB activation results in the attenuation of exaggerated catabolism and inflammatory reactions in FLSs. For decades, Andro has been reported to exert appropriate inhibitory effects on NF-κB activity [48] and suppress inflammation in various diseases [49], including neuroinflammation [50], enteritis [51] and psoriasis [52]. Studies have also demonstrated that Andro inhibits the production of matrix metalloproteinases and inducible nitric oxide [18], and protects chondrocytes from oxidative stress injury [19], which is significant for delaying cartilage degeneration in OA treatment. In this study, Andro reduced the phosphorylation of p65 in FLSs in a dose-dependent manner, indicating a potential mechanism related to the anti-inflammatory effect of Andro in OA synovitis for treating OA. Previous investigations have reported that the NF-κB signalling pathway plays a key role in facilitating TNFα functions [53]. TNFα induces cartilage lesions and synovial inflammation by binding to its receptors TNFR1 and TNFR2 [54,55]. TNFR1 is a strong inducer of proinflammatory activities, but TNFR2 can elicit both proinflammatory and anti-inflammatory effects in a variety of pathologies [56]. Based on the dual role of the TNFR2 system, the molecular mechanisms of TNFR2

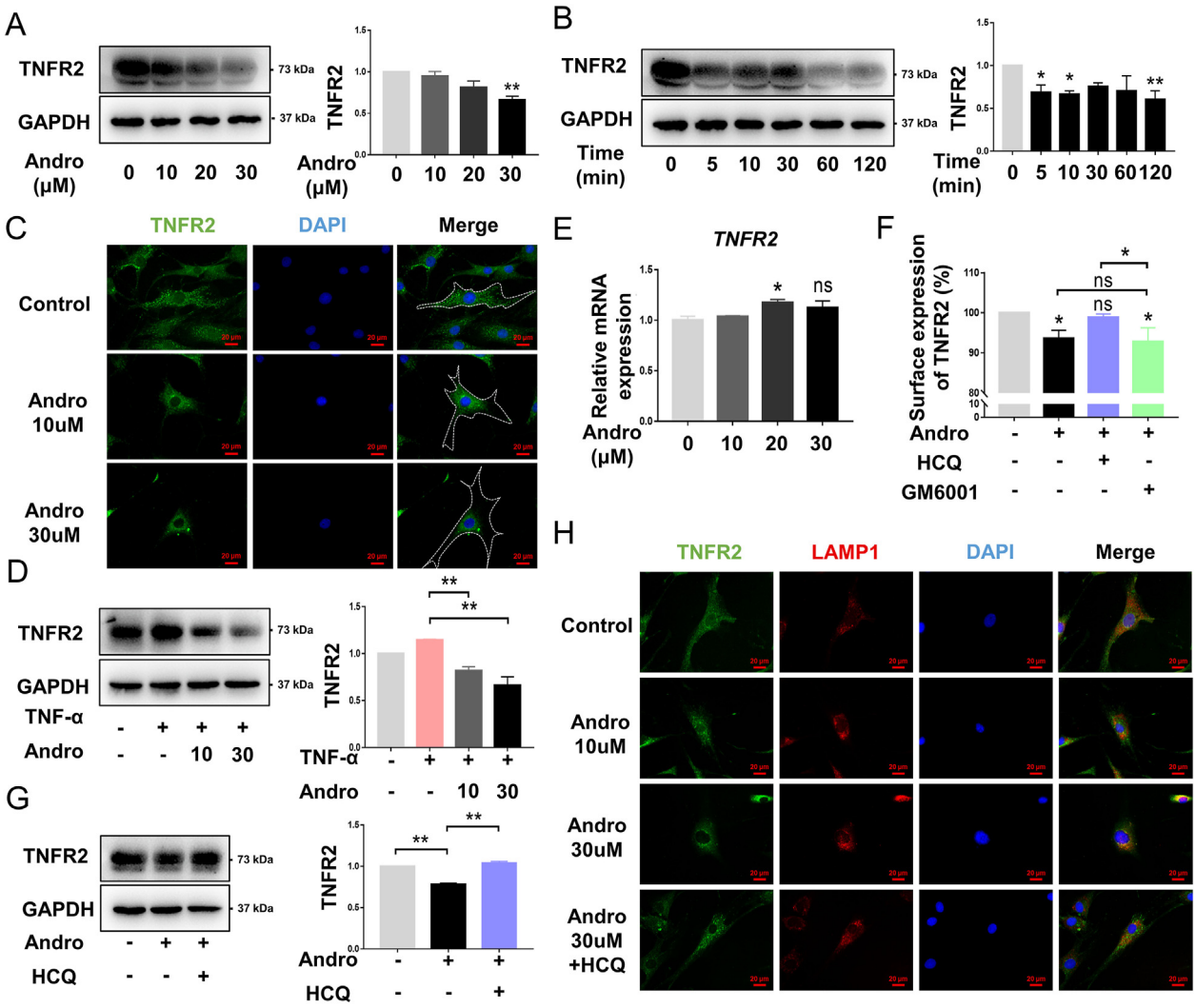

Fig. 4. Effects of Andro on TNFR2 *in vitro* (A) FLSs were treated with 0, 10, 20, and 30 μM Andro for 10 min, and the level of TNFR2 protein was assessed (n = 3) (B) FLSs were treated with 30 μM Andro for 0, 5, 10, 30, 60, and 120 min, and the level of TNFR2 protein was assessed (n = 3) (C) Representative fluorescent images of TNFR2 in FLSs under the treatment of Andro for 10 min (scale bar: 20 μm) (D) FLSs pretreated with 10 and 30 μM Andro for 1 h were stimulated with TNFα (10 ng/mL) for 10 min, and the level of TNFR2 protein was assessed (n = 3) (E) mRNA expression of TNFR2 during the treatment of FLSs with Andro for 10 min (n = 3) (F) Surface expression of TNFR2 after Andro treatment. The FLSs pretreated with HCQ (50 μM) and GM6001 (10 μM) for 1 h were incubated with Andro for 10 min, and surface TNFR2 was analyzed by flow cytometry. The mean fluorescence intensity of surface receptor levels is expressed as a percentage of vehicle control (n = 3) (G) The FLSs pretreated with HCQ (50 μM) for 1 h were incubated with Andro for 10 min, and the level of TNFR2 protein was assessed (n = 3) (H) Representative fluorescent images of TNFR2 co-localized with LAMP-1 in FLSs upon treatment with Andro for 10 min (scale bar: 20 μm). ns, $p > 0.05$, *$p < 0.05$; **$p < 0.01$.

regulation for the treatment of synovial inflammation is of significance. Silencing TNFR2 in FLSs decreased the phosphorylation of p65, and Andro reduced the expression of TNFR2. After reversing TNFR2 expression using HCQ, high levels of p65 phosphorylation, CCL2, ADAMTS4, and ADAMTS5 were observed in this study, which further demonstrates a correlation between TNFR2 and NF-κB signalling in the anti-inflammatory effects of Andro.

The present study has several limitations. First, the classic view of OA pathogenesis is that subchondral sclerosis is associated with joint degeneration [57]; however, the effects of Andro on subchondral bone remodelling were not investigated. Second, the effect of Andro on inflammation and the neuropeptide release of peptidergic fibres *in vitro* was not investigated. Third, recent studies have shown that signal transduction might result from endosomal/lysosomal compartments [58], but the mechanism underlying Andro-mediated regulation of synovial inflammation could not be identified. The process by which Andro regulates TNFR2 trafficking and the NF-κB signalling pathway also remains unclear. Endocytosis has been regarded as a mechanism to terminate signalling through receptor internalization and subsequent lysosomal degradation [20]. Although this study provides evidence that the inhibition of NF-κB signalling and inflammation by Andro is a response to the regulation of TNFR2 internalization and degradation, further studies are needed to elucidate the exact mechanism by which Andro induces TNFR2 endocytosis and inhibits NF-κB phosphorylation.

5. Conclusions

In summary, Andro reduces the NF-κB activation and inflammatory responses in synoviocytes via increased TNFR2 internalization and degradation. This is the first report on the inhibition of Andro on NF-κB activation by targeting TNFR2, and suggests that inhibition of both TNFR2 and Andro could be novel therapeutic approaches for OA and

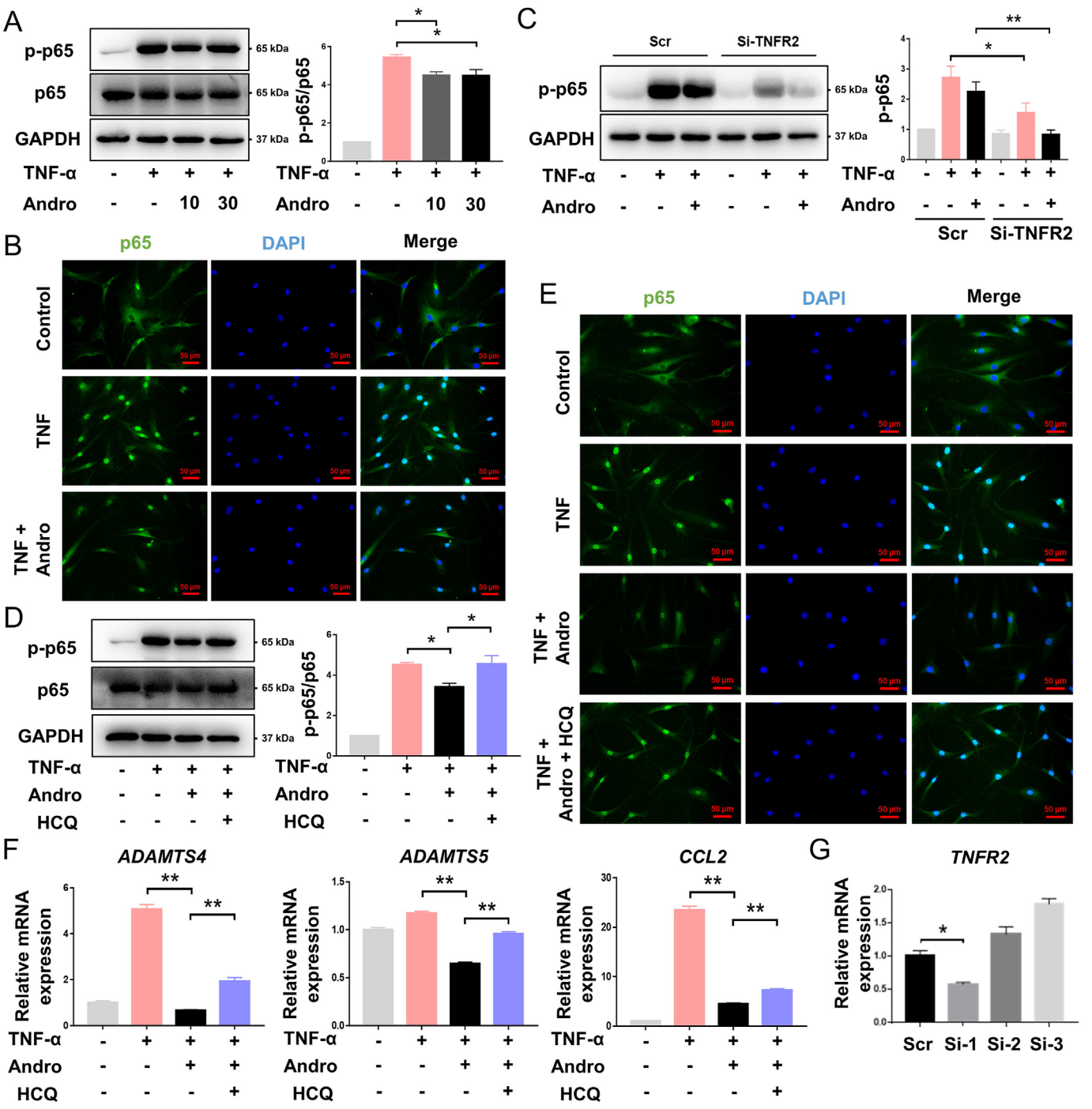

Fig. 5. Effects of Andro on NF-κB signaling *in vitro* (A) FLSs pretreated with 10 and 30 μM Andro for 1 h were stimulated with TNFα (10 ng/mL) for 10 min, and the level of NF-κB (p65) phosphorylation was assessed (n = 3) (B) Representative fluorescent images of nuclear translocation of p65 in FLSs as a response to stimulation of TNFα (10 ng/mL) with/without Andro (scale bar: 50 μm) (C) P65 phosphorylation in siTNFR2 cells was markedly impaired as compared to cells transduced with scrambled siRNAs (Scr) as a response to stimulation of TNFα (10 ng/mL) with/without Andro (n = 3) (D) FLSs were treated with Andro with/without HCQ for 1 h, stimulated with TNFα (10 ng/mL) for 10 min, and the levels of p65 phosphorylation assessed (n = 3) (E) Representative fluorescent images of nuclear translocation of p65 in FLSs under the stimulation of TNFα (10 ng/mL) with/without Andro and HCQ (scale bar: 50 μm) (F) After the stimulation of TNFα (10 ng/mL), mRNA expression of inflammatory cytokines in FLSs with/without Andro and HCQ for 24 h (n = 3) (G) qPCR analyses for *TNFR2* mRNA expression after FLSs were transfected with scrambled siRNAs (Scr) or siRNAs against TNFR2(n = 3). *p < 0.05; **p < 0.01.

pain.

Funding statement

This work was supported by National Key R&D Program of China (2018YFC1105904); Key Program of NSFC, China (81730067); National Science Foundation of China (81772335, 81941009, 81802196); Natural Science Foundation of Jiangsu Province, China (BK20180127); Jiangsu Provincial Key Medical Talent Foundation, China; Six Talent Peaks Project of Jiangsu Province, China (WSW-079).

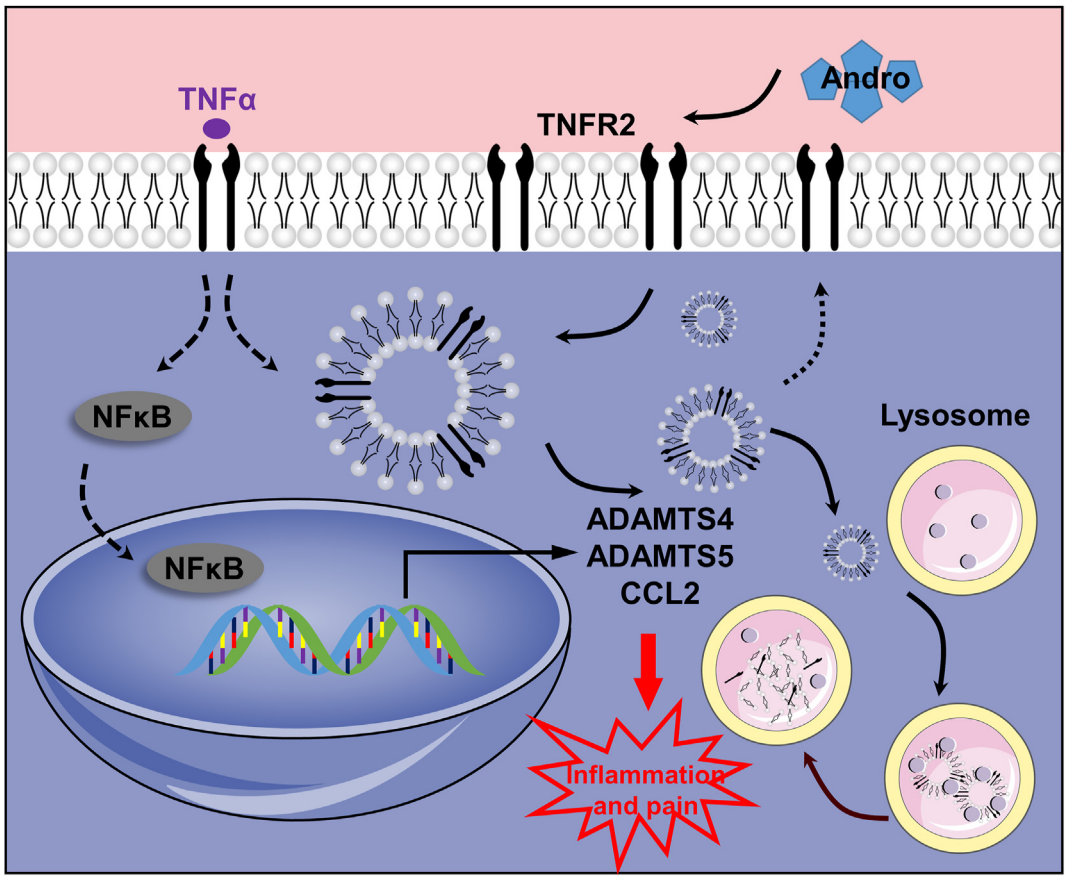

Fig. 6. Proposed mechanism of Andro-induced TNFR2 degradation. Inflammation produced in response to TNFα activates NF-κB signaling in FLSs by interacting with TNFR2. A proportion of TNFR2 enters the cell by endocytosis and is recycled back to the surface, whereas receptor trafficking from the late endosome to the lysosome is promoted after Andro treatment.

Authors' contributions

Rongliang Wang: Conceptualization, Methodology, Software, Validation, Formal analysis, Investigation, Writing - Original Draft, Visualization; **Jiawei Li**: Conceptualization, Methodology, Validation, Investigation; **Xingquan Xu**: Conceptualization, Supervision, Writing - Original Draft, Funding acquisition; **Jia Xu** : Methodology, Investigation; **Huiming Jiang:** Methodology, Investigation; **Zhongyang Lv**: Writing - Original Draft; **Rui Wu** : Investigation; **Ziying Sun**: Investigation; **Wenjie Guo**: Investigation; **Yang Sun**: Conceptualization, Supervision, Writing - Original Draft; **Shiro Ikegawa**: Supervision; **Qing Jiang**: Conceptualization, Supervision, Funding acquisition; **Dongquan Shi**: Conceptualization, Writing - Original Draft, Visualization, Supervision, Funding acquisition.

Declaration of competing interest

The authors have declared no conflicts of interest.

Acknowledgments

We thank the kind advice of our colleagues towards this study.

References

[1] Liu-Bryan R, Terkeltaub R. Emerging regulators of the inflammatory process in osteoarthritis. Nat Rev Rheumatol 2015;11(1):35–44.
[2] Bannuru RR, Osani MC, Vaysbrot EE, Arden NK, Bennell K, Bierma-Zeinstra SMA, et al. OARSI guidelines for the non-surgical management of knee, hip, and polyarticular osteoarthritis. Osteoarthritis Cartilage 2019;27(11):1578–89.
[3] Sellam J, Berenbaum F. The role of synovitis in pathophysiology and clinical symptoms of osteoarthritis. Nat Rev Rheumatol 2010;6(11):625–35.
[4] Bao J, Yan W, Xu K, Chen M, Chen Z, Ran J, et al. Oleanolic acid decreases IL-1beta-induced activation of fibroblast-like synoviocytes via the SIRT3-NF-kappaB Axis in osteoarthritis. Oxid Med Cell Longev 2020;2020:7517219.
[5] Mathiessen A, Conaghan PG. Synovitis in osteoarthritis: current understanding with therapeutic implications. Arthritis Res Ther 2017;19(1):18.
[6] Schaible HG, Ebersberger A, Von Banchet GS. Mechanisms of pain in arthritis. Ann N Y Acad Sci 2002;966:343–54.
[7] Saito T, Koshino T. Distribution of neuropeptides in synovium of the knee with osteoarthritis. Clin Orthop Relat Res 2000;(376):172–82.
[8] Marshall KW, Theriault E, Homonko DA. Distribution of substance P and calcitonin gene related peptide immunoreactivity in the normal feline knee. J Rheumatol 1994;21(5):883–9.
[9] Bonnet CS, Williams AS, Gilbert SJ, Harvey AK, Evans BA, Mason DJ, et al. AMPA/kainate glutamate receptors contribute to inflammation, degeneration and pain related behaviour in inflammatory stages of arthritis. Ann Rheum Dis 2015;74(1):242–51.
[10] Youn J, Kim HY, Park JH, Hwang SH, Lee SY, Cho CS, et al. Regulation of TNF-alpha-mediated hyperplasia through TNF receptors, TRAFs, and NF-kappaB in synoviocytes obtained from patients with rheumatoid arthritis. Immunol Lett 2002;83(2):85–93.
[11] Deleuran BW, Chu CQ, Field M, Brennan FM, Mitchell T, Feldmann M, et al. Localization of tumor necrosis factor receptors in the synovial tissue and cartilage-pannus junction in patients with rheumatoid arthritis. Implications for local actions of tumor necrosis factor alpha. Arthritis Rheum 1992;35(10):1170–8.
[12] Al-Azab M, Wei J, Ouyang X, Elkhider A, Walana W, Sun X, et al. TL1A mediates fibroblast-like synoviocytes migration and Indian Hedgehog signaling pathway via TNFR2 in patients with rheumatoid arthritis. Eur Cytokine Netw 2018;29(1):27–35.
[13] Borghi A, Haegman M, Fischer R, Carpentier I, Bertrand MJM, Libert C, et al. The E3 ubiquitin ligases HOIP and cIAP1 are recruited to the TNFR2 signaling complex and mediate TNFR2-induced canonical NF-kappaB signaling. Biochem Pharmacol 2018;153:292–8.
[14] Le Roy C, Wrana JL. Clathrin- and non-clathrin-mediated endocytic regulation of cell signalling. Nat Rev Mol Cell Biol 2005;6(2):112–26.
[15] Tchikov V, Bertsch U, Fritsch J, Edelmann B, Schutze S, et al. Subcellular compartmentalization of TNF receptor-1 and CD95 signaling pathways. Eur J Cell Biol 2011;90(6–7):467–75.

[16] Gao J, Peng S, Shan X, Deng G, Shen L, Sun J, et al. Inhibition of AIM2 inflammasome-mediated pyroptosis by Andrographolide contributes to amelioration of radiation-induced lung inflammation and fibrosis. Cell Death Dis 2019;10(12):957.
[17] Tran QTN, Wong WSF, Chai CLL. The identification of naturally occurring labdane diterpenoid calcaratarin D as a potential anti-inflammatory agent. Eur J Med Chem 2019;174:33–44.
[18] Ding QH, Ji XW, Cheng Y, Yu YQ, Qi YY, Wang XH, et al. Inhibition of matrix metalloproteinases and inducible nitric oxide synthase by andrographolide in human osteoarthritic chondrocytes. Mod Rheumatol 2013;23(6):1124–32.
[19] Li B, Jiang T, Liu H, Miao Z, Fang D, Zheng L, et al. Andrographolide protects chondrocytes from oxidative stress injury by activation of the Keap1-Nrf2-Are signaling pathway. J Cell Physiol 2018;234(1):561–71.
[20] Tan Y, Chiow KH, Huang D, Wong SH, et al. Andrographolide regulates epidermal growth factor receptor and transferrin receptor trafficking in epidermoid carcinoma (A-431) cells. Br J Pharmacol 2010;159(7):1497–510.
[21] Li JW, Wang RL, Xu J, Sun KY, Jiang HM, Sun ZY, et al. Methylene blue prevents osteoarthritis progression and relieves pain in rats via upregulation of Nrf2/PRDX1. Acta Pharmacol Sin 2021:1–12.
[22] Sun R, Zhang Z, Lei Y, Liu Y, Lu C, Rong H, et al. Hippocampal activation of microglia may underlie the shared neurobiology of comorbid posttraumatic stress disorder and chronic pain12. Mol Pain; 2016.
[23] Vuralli D, Wattiez AS, Russo AF, Bolay H, et al. Behavioral and cognitive animal models in headache research. J Headache Pain 2019;20(1):11.
[24] Ruan MZ, Patel RM, Dawson BC, Jiang MM, Lee BH, et al. Pain, motor and gait assessment of murine osteoarthritis in a cruciate ligament transection model. Osteoarthritis Cartilage 2013;21(9):1355–64.
[25] Faust HJ, Sommerfeld SD, Rathod S, Rittenbach A, Ray Banerjee S, Tsui BMW, et al. A hyaluronic acid binding peptide-polymer system for treating osteoarthritis. Biomaterials 2018;183:93–101.
[26] Gerwin N, Bendele AM, Glasson S, Carlson CS, et al. The OARSI histopathology initiative - recommendations for histological assessments of osteoarthritis in the rat. Osteoarthritis Cartilage 2010;18(Suppl 3):S24–34.
[27] Pelletier JP, Martel-Pelletier J, Abramson SB. Osteoarthritis, an inflammatory disease: potential implication for the selection of new therapeutic targets. Arthritis Rheum 2001;44(6):1237–47.
[28] Lauzier A, Charbonneau M, Harper K, Jilaveanu-Pelmus M, Dubois CM, et al. Formation of invadopodia-like structures by synovial cells promotes cartilage breakdown in collagen-induced arthritis: involvement of the protein tyrosine kinase Src. Arthritis Rheum 2011;63(6):1591–602.
[29] Rahmati M, Mobasheri A, Mozafari M. Inflammatory mediators in osteoarthritis: a critical review of the state-of-the-art, current prospects, and future challenges. Bone 2016;85:81–90.
[30] Verma P, Dalal K. ADAMTS-4 and ADAMTS-5: key enzymes in osteoarthritis. J Cell Biochem 2011;112(12):3507–14.
[31] Raghu H, Lepus CM, Wang Q, Wong HH, Lingampalli N, Oliviero F, et al. CCL2/CCR2, but not CCL5/CCR5, mediates monocyte recruitment, inflammation and cartilage destruction in osteoarthritis. Ann Rheum Dis 2017;76(5):914–22.
[32] Pan L, Zhang Y, Chen N, Yang L, et al. Icariin regulates cellular functions and gene expression of osteoarthritis patient-derived human fibroblast-like synoviocytes. Int J Mol Sci 2017;18(12).
[33] Connolly M, Veale DJ, Fearon U. Acute serum amyloid A regulates cytoskeletal rearrangement, cell matrix interactions and promotes cell migration in rheumatoid arthritis. Ann Rheum Dis 2011;70(7):1296–303.
[34] Li GF, Qin YH, Du PQ. Andrographolide inhibits the migration, invasion and matrix metalloproteinase expression of rheumatoid arthritis fibroblast-like synoviocytes via inhibition of HIF-1alpha signaling. Life Sci 2015;136:67–72.
[35] Jin Y, Smith C, Monteith D, Brown R, Camporeale A, McNearney TA, et al. CGRP blockade by galcanezumab was not associated with reductions in signs and symptoms of knee osteoarthritis in a randomized clinical trial. Osteoarthritis Cartilage 2018;26(12):1609–18.
[36] Kloefkorn HE, Jacobs BY, Loye AM, Allen KD, et al. Spatiotemporal gait compensations following medial collateral ligament and medial meniscus injury in the rat: correlating gait patterns to joint damage. Arthritis Res Ther 2015;17:287.
[37] Lluch E, Torres R, Nijs J, Van Oosterwijck J, et al. Evidence for central sensitization in patients with osteoarthritis pain: a systematic literature review. Eur J Pain 2014;18(10):1367–75.
[38] Chakrabarti S, Hore Z, Pattison LA, Lalnunhlimi S, Bhebhe CN, Callejo G, et al. Sensitization of knee-innervating sensory neurons by tumor necrosis factor-alpha-activated fibroblast-like synoviocytes: an in vitro, coculture model of inflammatory pain. 2020. Pain.
[39] Stoppiello LA, Mapp PI, Wilson D, Hill R, Scammell BE, Walsh DA, et al. Structural associations of symptomatic knee osteoarthritis. Arthritis Rheum 2014;66(11):3018–27.
[40] Bove SE, Laemont KD, Brooker RM, Osborn MN, Sanchez BM, Guzman RE, et al. Surgically induced osteoarthritis in the rat results in the development of both osteoarthritis-like joint pain and secondary hyperalgesia. Osteoarthritis Cartilage 2006;14(10):1041–8.
[41] Miller RE, Tran PB, Ishihara S, Larkin J, Malfait AM, et al. Therapeutic effects of an anti-ADAMTS-5 antibody on joint damage and mechanical allodynia in a murine model of osteoarthritis. Osteoarthritis Cartilage 2016;24(2):299–306.
[42] Miotla Zarebska J, Chanalaris A, Driscoll C, Burleigh A, Miller RE, Malfait AM, et al. CCL2 and CCR2 regulate pain-related behaviour and early gene expression in post-traumatic murine osteoarthritis but contribute little to chondropathy. Osteoarthritis Cartilage 2017;25(3):406–12.
[43] Fotin-Mleczek M, Welte S, Mader O, Duchardt F, Fischer R, Hufnagel H, et al. Cationic cell-penetrating peptides interfere with TNF signalling by induction of TNF receptor internalization. J Cell Sci 2005;118(Pt 15):3339–51.
[44] Reddy P, Slack JL, Davis R, Cerretti DP, Kozlosky CJ, Blanton RA, et al. Functional analysis of the domain structure of tumor necrosis factor-alpha converting enzyme. J Biol Chem 2000;275(19):14608–14.
[45] Zhou H, Ding G, Liu W, Wang L, Lu Y, Cao H, et al. Lipopolysaccharide could be internalized into human peripheral blood mononuclear cells and elicit TNF-alpha release, but not via the pathway of toll-like receptor 4 on the cell surface. Cell Mol Immunol 2004;1(5):373–7.
[46] Fischer R, Maier O, Naumer M, Krippner-Heidenreich A, Scheurich P, Pfizenmaier K, et al. Ligand-induced internalization of TNF receptor 2 mediated by a di-leucin motif is dispensable for activation of the NFkappaB pathway. Cell Signal 2011;23(1):161–70.
[47] Eskelinen EL, Tanaka Y, Saftig P. At the acidic edge: emerging functions for lysosomal membrane proteins. Trends Cell Biol 2003;13(3):137–45.
[48] Bao Z, Guan S, Cheng C, Wu S, Wong SH, Kemeny DM, et al. A novel antiinflammatory role for andrographolide in asthma via inhibition of the nuclear factor-kappaB pathway. Am J Respir Crit Care Med 2009;179(8):657–65.
[49] Tan WSD, Liao W, Zhou S, Wong WSF, et al. Is there a future for andrographolide to be an anti-inflammatory drug? Deciphering its major mechanisms of action. Biochem Pharmacol 2017;139:71–81.
[50] Li X, Wang T, Zhang D, Li H, Shen H, Ding X, et al. Andrographolide ameliorates intracerebral hemorrhage induced secondary brain injury by inhibiting neuroinflammation induction. Neuropharmacology 2018;141:305–15.
[51] Guo W, Sun Y, Liu W, Wu X, Guo L, Cai P, et al. Small molecule-driven mitophagy-mediated NLRP3 inflammasome inhibition is responsible for the prevention of colitis-associated cancer. Autophagy 2014;10(6):972–85.
[52] Shao F, Tan T, Tan Y, Sun Y, Wu X, Xu Q, et al. Andrographolide alleviates imiquimod-induced psoriasis in mice via inducing autophagic proteolysis of MyD88. Biochem Pharmacol 2016;115:94–103.
[53] Rosebeck S, Rehman AO, Apel IJ, Kohrt D, Appert A, O'Donnell MA, et al. The API2-MALT1 fusion exploits TNFR pathway-associated RIP1 ubiquitination to promote oncogenic NF-kappaB signaling. Oncogene 2014;33(19):2520–30.
[54] Yamamoto K, Okano H, Miyagawa W, Visse R, Shitomi Y, Santamaria S, et al. MMP-13 is constitutively produced in human chondrocytes and co-endocytosed with ADAMTS-5 and TIMP-3 by the endocytic receptor LRP1. Matrix Biol 2016;56:57–73.
[55] Lotzer K, Dopping S, Connert S, Grabner R, Spanbroek R, Lemser B, et al. Mouse aorta smooth muscle cells differentiate into lymphoid tissue organizer-like cells on combined tumor necrosis factor receptor-1/lymphotoxin beta-receptor NF-kappaB signaling. Arterioscler Thromb Vasc Biol 2010;30(3):395–402.
[56] Medler J, Wajant H. Tumor necrosis factor receptor-2 (TNFR2): an overview of an emerging drug target. Expert Opin Ther Targets 2019;23(4):295–307.
[57] Burr DB, Gallant MA. Bone remodelling in osteoarthritis. Nat Rev Rheumatol 2012;8(11):665–73.
[58] Schutze S, Tchikov V, Schneider-Brachert W. Regulation of TNFR1 and CD95 signalling by receptor compartmentalization. Nat Rev Mol Cell Biol 2008;9(8):655–62.